Received: 9 August 2021 | Revised: 28 October 2021 | Accepted: 28 October 2021

DOI: 10.1111/xen.12719

Xenotransplantation WILEY

ORIGINAL ARTICLE

Transgenic pigs expressing near infrared fluorescent protein—A novel tool for noninvasive imaging of islet xenotransplants

Elisabeth Kemter[1,2,3] | Antonio Citro[4] | Lelia Wolf-van Buerck[5] | Yi Qiu[6] | Anika Böttcher[3,7] | Martina Policardi[4] | Silvia Pellegrini[4] | Libera Valla[1,2,8] | Marianna Alunni-Fabbroni[9] | Julianna Kobolák[10] | Barbara Kessler[1,2] | Mayuko Kurome[1,2] | Valeri Zakhartchenko[1,2] | Andras Dinnyes[10] | Clemens C. Cyran[9] | Heiko Lickert[3,7] | Lorenzo Piemonti[4,11] | Jochen Seissler[5] | Eckhard Wolf[1,2,3]

[1] Department of Veterinary Sciences and Gene Center, Chair for Molecular Animal Breeding and Biotechnology, LMU Munich, Munich, Germany

[2] Department of Veterinary Sciences, Center for Innovative Medical Models (CiMM), LMU Munich, Oberschleißheim, Germany

[3] German Center for Diabetes Research (DZD), Neuherberg, Germany

[4] San Raffaele Diabetes Research Institute, IRCCS Ospedale San Raffaele, Milan, Italy

[5] Diabetes Center, Medical Clinic and Policlinic IV, University Hospital, LMU Munich, Munich, Germany

[6] iThera Medical, Munich, Germany

[7] Institute of Diabetes and Regeneration Research, Helmholtz Zentrum München, Neuherberg, Germany

[8] MWM Biomodels GmbH, Tiefenbach, Germany

[9] Department of Radiology, University Hospital, LMU Munich, Munich, Germany

[10] BioTalentum Ltd., Gödöllö, Hungary

[11] Vita-Salute San Raffaele University, Milan, Italy

Correspondence
Elisabeth Kemter, Chair for Molecular Animal Breeding and Biotechnology, Gene Center and Department of Veterinary Sciences, LMU Munich, 81377 Munich, Germany.
Email: kemter@genzentrum.lmu.de
Eckhard Wolf, Center for Innovative Medical Models (CiMM), Department of Veterinary Sciences, LMU Munich, 85764 Oberschleißheim, Germany.
Email: ewolf@genzentrum.lmu.de

Jochen Seissler and Eckhard Wolf contributed equally to this work.

Abstract

Background: Islet xenotransplantation is a promising concept for beta-cell replacement therapy. Reporter genes for noninvasive monitoring of islet engraftment, graft mass changes, long-term survival, and graft failure support the optimization of transplantation strategies. Near-infrared fluorescent protein (iRFP) is ideal for fluorescence imaging (FI) in tissue, but also for multispectral optoacoustic tomography (MSOT) with an even higher imaging depth. Therefore, we generated reporter pigs ubiquitously expressing iRFP.

Methods: CAG-iRPF720 transgenic reporter pigs were generated by somatic cell nuclear transfer from FACS-selected stable transfected donor cells. Neonatal

Abbreviations: BLI, bioluminescence imaging; CAG, cytomegalovirus early enhancer element, chicken beta-actin gene promoter, first exon and first intron, splice acceptor of the rabbit beta-globin gene; FACS, fluorescence activated cell sorting; FI, fluorescence imaging; IPGTT, intraperitoneal glucose tolerance test; iRFP, near-infrared fluorescent protein; MRI, magnetic resonance imaging; MSOT, multispectral optoacoustic tomography; NPI, neonatal pig islet; NSG, NOD-*scid* IL2Rg^{null}; ROI, region of interest; SCNT, somatic cell nuclear transfer; SPECT, single photon emission computed tomography; SPIO, superparamagnetic iron oxide nanoparticle

Funding information
European Union's Horizon 2020, Grant/Award Number: 760986; Marie Skłodowska Curie, Grant/Award Number: 812660; Deutsche Forschungsgemeinschaft, Grant/Award Number: TRR127; Bayerische Forschungsstiftung, Grant/Award Number: 1247-16; German Centre for Diabetes Research, Grant/Award Number: 82DZD00802; H2020 Industrial Leadership, Grant/Award Number: 760986

pig islets (NPIs) were transplanted into streptozotocin-diabetic immunodeficient NOD-*scid* IL2Rg^{null} (NSG) mice. FI and MSOT were performed to visualize different numbers of NPIs and to evaluate associations between signal intensity and glycemia. MSOT was also tested in a large animal model.

Results: CAG-iRFP transgenic NPIs were functionally equivalent with wild-type NPIs. Four weeks after transplantation under the kidney capsule, FI revealed a twofold higher signal for 4000-NPI compared to 1000-NPI grafts. Ten weeks after transplantation, the fluorescence intensity of the 4000-NPI graft was inversely correlated with glycemia. After intramuscular transplantation into diabetic NSG mice, MSOT revealed clear dose-dependent signals for grafts of 750, 1500, and 3000 NPIs. Dose-dependent MSOT signals were also revealed in a pig model, with stronger signals after subcutaneous (depth ~6 mm) than after submuscular (depth ~15 mm) placement of the NPIs.

Conclusions: Islets from CAG-iRFP transgenic pigs are fully functional and accessible to long-term monitoring by state-of-the-art imaging modalities. The novel reporter pigs will support the development and preclinical testing of novel matrices and engraftment strategies for porcine xeno-islets.

KEYWORDS
imaging, islet, pig, xenotransplantation

1 | INTRODUCTION

Xenotransplantation of porcine pancreatic islets is a promising approach for the treatment of patients with insulin-deficient diabetes mellitus. The optimization of strategies to improve islet engraftment and long-term survival is an active field of preclinical research (reviewed in Ref. 1), which would markedly benefit from the possibility of noninvasive monitoring of the islet transplants. Circulating C-peptide, insulin, and glucose levels provide only indirect estimates of islet mass and graft fate.[2]

The use of neonatal pig islets (NPI) from an *INS*-eGFP reporter line[3] facilitated longitudinal studies of beta-cell mass expansion and islet vascularization after transplantation into the anterior chamber of the mouse eye.[4] At other transplantations sites, the eGFP signal is absorbed by overlaying tissue and additionally disturbed by autofluorescence of endogenous chromogens. Since light has its maximum penetration in tissue in the near-infrared (NIR) optical window (~650–900 nm) (reviewed in Refs. 5,6), fluorophores with emission and excitation wavelengths in this range are ideal for fluorescence imaging (FI) of islet grafts in rodent models. Due to the small imaging depth, FI is limited in large animal models.

Multispectral optoacoustic tomography (MSOT) is a noninvasive imaging modality combining ultrasound and optoacoustic imaging (reviewed in Ref. [7]). Tissue is exposed to pulsed multiwavelength laser light. Absorption by chromophores (e.g., hemoglobin, lipids, melanin, collagens) creates thermally induced ultrasonic pressure waves, which are received by acoustic detectors to form images. Spectral unmixing allows the quantification of specific chromophores based on their specific absorption and reflection properties (reviewed in Ref. [8]). Due to its penetration depth of up to 5 cm, MSOT allows also topical transcutaneous imaging in large animal models (reviewed in Ref. [9]). Moreover, cells or tissues can be engineered to express exogenous chromophores like near-infrared fluorescent protein (iRFP) for longitudinal noninvasive monitoring of their fate after transplantation. Therefore, we generated transgenic pigs expressing iRFP720[10] and tested noninvasive imaging of their pancreatic islets after transplantation into small and large recipient animals.

2 | MATERIALS AND METHODS

All experiments involving animals were approved by the responsible authorities (district governments of Upper Bavaria, Germany, and of Milan, Italy) and were conducted in accordance with Directive 2010/63/EU and with the German and Italian Animal Welfare Acts.

2.1 | Generation of CAG-iRFP transgenic pigs

An expression cassette for iRFP720 under the control of a ubiquitously active CAG regulatory sequence (Figure 1A) was released from plasmid pCAG-iRFP720 (Addgene #89687[11]) and nucleofected into male porcine kidney cells.[12] Seven days after nucleofection, iRFP720 expressing kidney cells were selected by fluorescence activated cell sorting (FACS) and cultured for additional few days until 90% confluence before they were cryopreserved. An aliquot of FACS selected

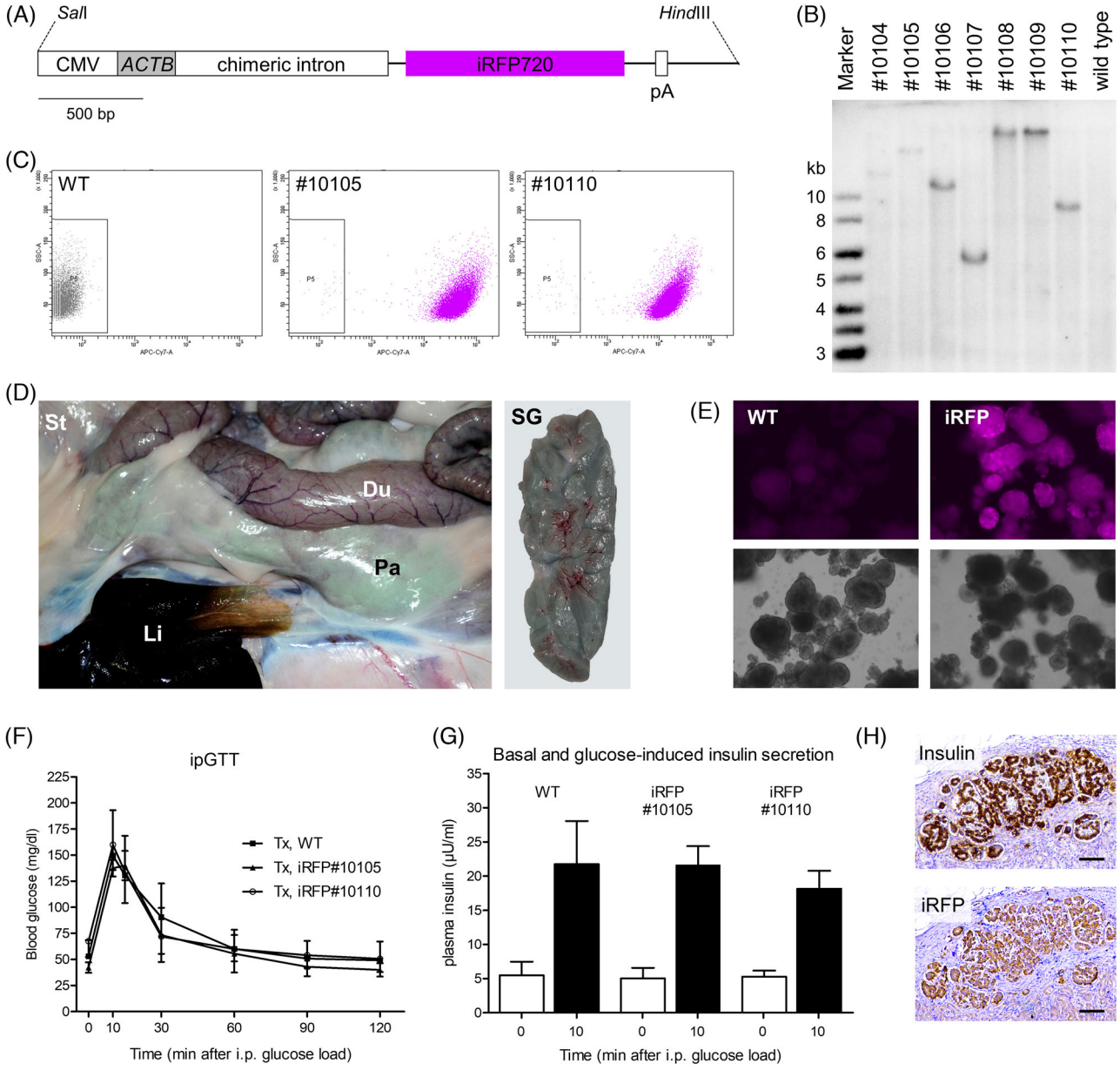

FIGURE 1 Characterization of CAG-iRFP transgenic pigs. (A) CAG-iRFP expression vector. CMV = cytomegalovirus enhancer; *ACTB* = chicken beta actin promoter; pA = rabbit beta globin polyadenylation signal. (B) Southern blot analysis of founder animals. Genomic DNA from tail tip samples was hydrolyzed with *Eco*RI (no restriction site in the CAG-iRFP720 fragment). The ^{32}P-labeled iRFP720 sequence served as probe. (C) FACS blots of skin cells to show expression intensity of iRFP720 of founder animals #10105 and #10110. (D) Greenish color of organs observed in macroscopic anatomy, representatively shown in an offspring of #10105. Du, duodenum; Li, liver; Pa, pancreas; SG, salivary gland; St, stomach. (E) iRFP fluorescence of isolated CAG-iRFP transgenic NPIs; WT = wild-type control. (F,G) Functional study of NPI transplants in vivo 4 months after transplantation of 3000 NPIs under the kidney capsule in streptozotocin (STZ)-diabetic immunodeficient NOD-*scid* IL2Rg^{null} (NSG) mice. (F) Intraperitoneal glucose tolerance test (ipGTT). (G) Basal and glucose-induced insulin secretion. (F, G) mean ± SD, n = 5 mice with NPI transplant of WT versus CAG-iRFP#10110 transgenic NPIs, and n = 4 mice with CAG-iRFP#10105 transgenic NPI transplant; no significance between genotype using one-way ANOVA. (H) Immunohistochemical staining of insulin and iRFP in sections from the subcapsular transplantation site 4 months after NPI CAG-iRFP#10105 transplantation

cells was propagated for 9 days before cells were re-evaluated for iRFP expression by flow cytometry. Subsequently, the pool of iRFP720 expressing kidney cells was used for somatic cell nuclear transfer (SCNT).[13] A total of 294 SCNT embryos were transferred laparoscopically into two estrous cycle-synchronized recipient gilts, resulting in one pregnancy and the birth of seven piglets. Transgenic founder animals were identified by PCR using primers iRFP_for 3′- AGCCTGACCTCTTGACCTGCG -5′ and iRFP_rev 3′- TGCAGGCCTAGTTTTGACTCGAC -5′. The transgene integration pattern of the founder animals was analyzed by Southern blot analysis of genomic DNA from tail tip samples, which was hydrolyzed with *Eco*RI (no restriction site in the CAG-iRFP720 fragment). The ^{32}P-labeled iRFP720 sequence served as

probe. Selected founder boars were mated with wild-type (WT) sows to establish transgenic lines.

2.2 | Isolation of neonatal pancreatic islets and xenotransplantation into mouse models

Neonatal pancreatic islets (NPIs) were isolated from 1- to 6-day-old piglets as described previously.[3] Briefly, for NPI isolates for FI, pancreas pieces were digested by collagenase-V (Sigma-Aldrich) and the released NPIs and clusters of exocrine cells cultured at 37°C for 3 days in recovery medium (Ham's F12/M199 with protease inhibitors, antioxidants, and additional nutrients). Full media change was carried out at days 1 and 3 postisolation to remove exocrine cells. Overnight shipment of NPI isolates from Munich to Milan was done in 50-mL tubes in recovery medium at room temperature. Upon arrival in Milan, NPIs were subsequently maintained in maturation medium [Ham's F10, 10 mmol/L glucose, 50 μmol/L 3-isobutyl-1-methylxanthine, 0.5% [wt/vol] BSA, 2 mmol/L L-glutamine, 10 mmol/L nicotinamide (Sigma-Aldrich, Germany), and 1% [vol/vol] penicillin/streptomycin stock (Gibco, Germany)] for additional 3 days, with half media change every other day. Streptozotocin (STZ, single dose of 180 mg/kg body weight)-diabetic immunodeficient NOD-*scid* IL2Rg^{null} (NSG) received each 1000 or 4000 iRFP720-tg NPIs transplanted under the kidney capsule, to monitor the islet xenograft by FI in Milan at the time points as indicated.

NPIs, which were transplanted for ipGTT analysis and MSOT imaging, were isolated by digestion of pancreas pieces using collagenase NB 6 (Nordmark Biochemicals), and cultured at 37°C in RPMI 1640 (PAN-Biotech, Germany) supplemented with 2% human serum albumin (Takeda, Germany), 10 mmol/L nicotinamide, 20 nmol/L exendin-4 (Sigma-Aldrich), and 1% Antibiotic-Antimycotic (Gibco, Germany). After 5–6 days, 3000 NPIs were either transplanted under the kidney capsule[14] or into the lower hind limb muscles[15] of STZ-diabetic-immunodeficient NSG mice. Blood glucose levels were monitored once daily (FreeStyle Lite; Abbott, Wiesbaden, Germany) and severely diabetic mice received daily insulin injections (0.25 to 1 U insulin glargine; Sanofi-Aventis) until blood glucose levels decreased to <300 mg/dL. After establishment of normoglycemia (random blood glucose level persistently <120 mg/dL), an intraperitoneal glucose tolerance test (ipGTT) was performed (2 g glucose/kg body weight) after a 5-h fasting period. Blood was collected from the tail vein at 0, 10, 30, 60, 90, and 120 min to measure blood glucose levels and insulin secretion using a porcine insulin ELISA (Mercodia, Uppsala, Sweden) according to the manufacturer's instruction. When a normal glucose tolerance was confirmed, mice were used for MSOT imaging (3-4 months after transplantation). After necropsy of the normoglycemic recipient mice, histological sections of the transplantation sites were stained by immunohistochemistry for insulin (guinea pig anti-insulin; 1:500; Dako, Hamburg, Germany) and iRFP (rabbit polyclonal tRFP antibody, 1:200, Evrogen JSC, Moscow, Russia). Bound antibodies were detected with horseradish peroxidase-conjugated secondary antibodies (Dako) and 3,3′-diaminobenzidine as chromogen.

In a second approach, for evaluation of MSOT imaging sensitivity of minimal transplant mass in the lower hind limb muscles in mice, a total of 300, 750, 1500, and 3000 iRFP720-tg NPIs, respectively, were injected per transplantation site and imaged 2 days post-transplantation. As negative controls, lower hind limb muscles of mice received PBS placebo or 1500 and 3000 WT NPIs, respectively. NPI transplantations were performed each in duplicated in regard of NPI genotype and transplant mass. Of note, defining region of interest (ROI) in MSOT imaging in each one iRFP transplant of 300 and 750 NPIs, respectively, was not feasible. In one hind leg, where 1500 WT NPIs were applied, a hematoma occurred, leading to exclusion of MSOT imaging measurement.

2.3 | Fluorescence imaging (FI)

In vivo FI was performed using an IVIS® SpectrumCT bioluminescent in vivo imaging system (PerkinElmer) calibrated to enable absolute quantitation of the bioluminescent signal and longitudinal studies can be performed over many time points. For this, iRFP NPIs transplanted under the kidney capsule were acquired by placing the NSG recipient mice at 37°C under gaseous anesthesia (2–3% isoflurane and 1 L/min oxygen). The IVIS SpectrumCT System (Perkin Elmer) was equipped with a low noise, back-thinned, back-illuminated CCD camera cooled at −90°C and with a quantum efficiency in the visible range >85%. Images were obtained using the following settings: exposure time = auto, binning = 8, f = 2, and a field-of-view equal to 13 cm (field C); when needed spectral unmixing, was obtained using the following excitation/emission filters: 640/680, 640/700, 640/720, 640/740, 640/760, 675/720, 675/740, 675/760, 675/780, 675/800 nm. To track the persistency of iRFP signal, graft FIs were acquired at the indicated time points post-transplantation of same graft recipients receiving 4000 NPIs under the kidney capsule. Image analyses were carried out considering two similar ROIs, one placed over the kidney (Tiss) and a background (Bk) region near the kidney. The radiant efficiency within these ROIs was measured using images acquired with the 675/720 filters. The tissue to background ratio TB(ti) was then calculated at different time points (ti) as follows: TB(ti) = [Tiss(ti))/(Bk(ti)]. Spectral unmixing of the FI data was performed on selected time points to show the specificity of the fluorescence signal over the tissue autofluorescence. All the images were acquired and analyzed using Living Image 4.5 (Perkin Elmer).

2.4 | Multispectral optoacoustic tomography (MSOT)

Mice with intramuscular CAG-iRFP NPI transplants in the legs were scanned with an MSOT inVision 256 small animal scanner (iThera Medical, Munich, Germany). After depilation of the leg region, anesthetized mice were positioned into the MSOT apparatus. The leg region was scanned with a step size of 0.3 mm. Optoacoustic signals from 680, 685, 695, 700, 705, 710, 715, 730, 760, 800, 850, 875 nm were acquired. Signal was averaged over 10 consecutive laser pulses for each

wavelength. Data analysis was performed using viewMSOT 4.0 software (iThera Medical). Backprojection algorithm was used for image reconstruction. Linear regression algorithm was used to spectrally unmix for iRFP, oxyhemoglobin, and deoxyhemoglobin. For quantifying the iRFP signal, equal sizes of regions of interest (ROI) were drawn in transplanted leg and the control leg. Mean signal intensity in the ROIs was quantified.

To study the applicability of detection of iRFP-expressing NPIs in a large animal model, plastic straws with a diameter of 3 mm were filled with a pipette at a density of 66,800, 17,580, and 8,350 NPIs per milliliters, respectively, after one end of the straws was first sealed with glue. Entrapped air in the straws was removed by short centrifugation. Subsequently, the straws were shortened with a scissor and the open end was sealed with glue. For mimicking in vivo imaging conditions but without animal distress, a 14-week-old pig was euthanized and its belly region was immediately cleaned and shaved. The NPI containing straws were surgically (via a median cut in the line alba) transplanted either subcutaneously or below the *M. rectus abdominis* (distance between straws and skin surface: 0.6 and 1.5 cm, respectively). For MSOT imaging, a handheld probe of 4 MHz center frequency was used in combination with the MSOT Acuity Echo research imaging system (iThera Medical). Optoacoustic signals from 680, 685, 695, 700, 705, 710, 715, 730, 760, 800, 850, 875 nm were acquired. Signal was averaged over seven consecutive laser pulses for each wavelength. In addition to optoacoustic imaging, interleaved ultrasound imaging (reflection-mode ultrasound computed tomography) was intergraded in the imaging system. Ultrasound images were used to assess the anatomical background for finding the straws. For data analysis, backprojection algorithm was used for image reconstruction; linear regression algorithm was used to spectrally unmix for iRFP720, oxyhemoglobin, and deoxyhemoglobin. All analysis was performed using iLabs software (iThera Medical). For quantifying the iRFP signal, circular ROIs were drawn around the straws using the ultrasound image. Mean iRFP optoacoustic signal intensity of the top 10% pixels in the ROIs was quantified.

3 | RESULTS

3.1 | Generation of CAG-iRFP transgenic pigs

Seven CAG-iRFP transgenic piglets were born of a SCNT pregnancy. Southern blot analysis revealed different integration sites of the CAG-iRFP expression cassette (Figure 1B). The level of transgene expression was assessed by MSOT of back skin[16] and by FACS analysis of skin cells from an ear biopsy. All seven founder animals showed iRFP expression at different levels (Supporting information Figure S1). Two founders (#10105, #10110) with consistent high-level iRFP expression (Figure 1C) were mated with WT sows and their progeny were used for further experiments. Upon necropsy of CAG-iRFP transgenic pigs, several organs, in particular salivary gland and pancreas, showed green color even under daylight (Figure 1D, offspring of founder #10105).

3.2 | NPIs from CAG-iRFP transgenic pigs are fully functional

NPIs isolated from CAG-iRFP transgenic piglets revealed bright fluorescence when analyzed by fluorescence microscopy (Figure 1E). Beta-cell function of iRFP transgenic (lines #10110 and #10105) and WT NPIs was tested by ipGTT in STZ-diabetic- immunodeficient NSG mice, which received 3000 NPIs transplanted under the kidney capsule. After an engraftment and maturation period of the NPI transplant of 4 months, percentage of mice developing normoglycemia, area under glucose curve, and insulin secretory capacity were similar in all groups (Figure 1F,G), indicating that iRFP transgenic NPI grafts of both lines are functionally equivalent with WT NPI grafts. Immunohistochemical analyses of sections from the subcapsular transplantation site of these mice showed large insulin-positive cell clusters that—in case of iRFP transgenic islets—also expressed iRFP (Figure 1H).

3.3 | Detection of CAG-iRFP transgenic NPIs by FI in vivo

We tested the suitability of iRFP720 reporter gene expression to monitor the fate of NPI xenotransplants in mice in vivo by FI using an IVIS® SpectrumCT bioluminescent in vivo imaging system. As iRFP transgene expression did not interfere with NPI graft function, NPIs from the high expressing line #10105 were used. STZ-diabetic NSG mice received either 1000 (n = 3) or 4000 (n = 4) NPIs under the kidney capsule, and FI was performed 4 weeks after transplantation in both groups, as well as 10 weeks after transplantation in the 4000 NPI-group. Four weeks after transplantation, the fluorescence signal in the 4000 NPI-group was twofold higher than in the 1000 NPI-group (Figure 2A). Of note, in the group receiving 4000 NPIs (n = 3; 1 recipient lost at week 5), the fluorescence intensity of the graft 10 weeks after transplantation was inversely correlated with glycemia (Figure 2B,C).

3.4 | Detection of CAG-iRFP transgenic NPI xenografts by MSOT in a small animal model

First, as proof of concept, MSOT imaging of intramuscularly (left hind limb) transplanted iRFP-tg NPIs was performed in four STZ-diabetic NSG mice after restoration of normoglycemia (3–4 months after transplantation). In all mice, a clear iRFP signal was detected in the graft bearing leg, whereas the control leg revealed almost no signal. 2D cross-sectional (Figure 3A) and 3D images (Figure 3B) of the leg show that the iRFP signal matches the NPI transplantation site. Quantification of the iRFP signal depicts the differences in the leg with the xenograft and the control leg (Figure 3C).

To estimate the sensitivity of MSOT, different amounts of iRFP NPIs were transplanted into hindlimb muscle of NSG mice and imaging was performed 2 days later (Figure 3D,E). The MSOT signal intensity of a 300 iRFP NPI transplant was in the range of the background

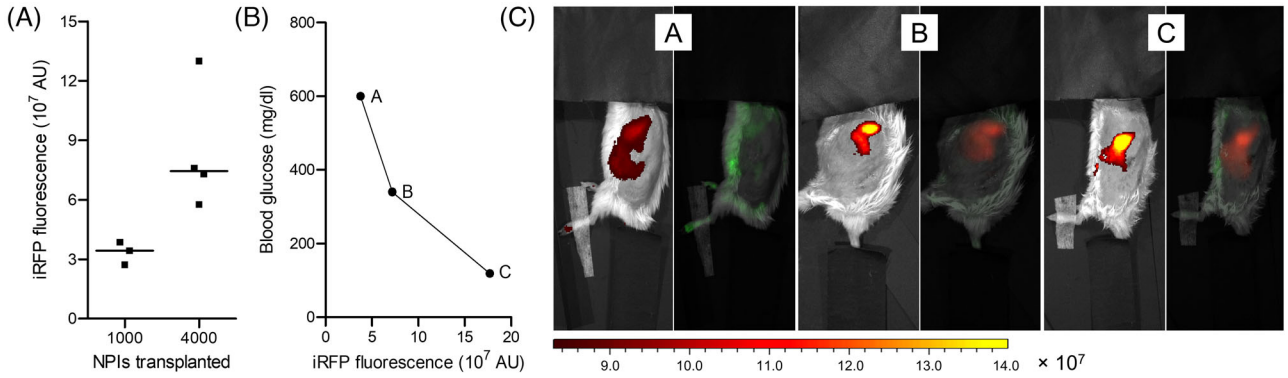

FIGURE 2 IVIS SpectrumCT in vivo fluorescence imaging of iRFP expressing NPI transplants in a small recipient model. (A) Quantification of fluorescence signal at 4 weeks after subcapsular transplantation of 1000 or 4000 iRFP720-tg NPIs in streptozotocin (STZ)-diabetic immunodeficient NOD-*scid* IL2Rg^{null} (NSG) mice for detection of graft mass in the graft expansion period. (B) Blood glucose concentration and quantified fluorescence signal at 10 weeks after transplantation of 4000 iRFP720-tg NPIs under the kidney capsule in three diabetic NSG mice. The grafts of these three mice were also in vivo imaged at 4 weeks after transplantation (A). (C) Fluorescence images of iRFP NPI grafts acquired with IVIS SpectrumCT System in three mice at 10 weeks after transplantation, differing in their blood glucose concentration. Left side: image of pure iRFP signal detection, right side: un-mixed image

signal of WT transplants (1500 or 3000 NPIs; Figure 3E). In contrast, the MSOT signal of a 750 iRFP NPI transplant was already clearly above this background. A further dose-dependent increase in MSOT signal was observed after transplantation of 1500 or 3000 NPIs (Figure 3E).

3.5 | Detection of CAG-iRFP NPI xenografts by MSOT in a large animal model

To assess the applicability of MSOT imaging in a large animal model, iRFP720-tg NPIs were filled into straws in predefined volume densities, and these straws were placed under the skin or the abdominal muscle of the belly of a freshly euthanized pig (Figure 4). The higher the NPIs density in straws, the higher signal intensities were monitored by MSOT imaging. MSOT signal intensity was dependent on the depth of the iRFP islets in the tissue with higher intensities at the subcutaneous site compared to the submuscular transplant site.

4 | DISCUSSION

Noninvasive monitoring of the islet transplants in vivo is an essential tool to understand islet engraftment as well as graft failure processes, as means to improve islet transplantation therapy. Several tools to image islet grafts in vivo were developed, exhibiting pros and cons (reviewed in Ref. [17]). For instance, single photon emission computed tomography (SPECT) and PET were successfully applied for imaging of islet grafts in small animal models and humans with high sensitivity, but require radiotracers and are locally limited to nuclear medicine facilities. Islets, labeled prior transplantation with superparamagnetic iron oxide nanoparticles (SPIOs), were successfully imaged by magnetic resonance imaging (MRI) also some weeks post-transplantation. However, when SPIOs were released from dying islets, it remains in the tissue and it cannot be differentiated if MRI signals were originating from live versus dead implants versus free SPIOs. Widely used in graft imaging are bioluminescence (BLI) and fluorescence (FI) imaging, but their application is limited to small animal models. For BLI, besides the need for luciferase transgene expression in the targeted cells, additional exogenous D-luciferin substrate has to be injected prior imaging. BLI was reported to be useful primarily for quantification rather than imaging of transplanted islets.[18]

In this study, we generated a transgenic pig overexpressing iRFP for imaging of grafted tissues. We demonstrated for the first time to our knowledge that iRFP-expressing pig islet grafts, which are fully functional, can be used to quantify graft mass not only by IF, but also by MSOT, therefore, by two complementary imaging modalities. Reporter islets-expressing iRFP can be used for evaluating islet engraftment, graft mass changes, long-term survival, and graft failure at new transplantation sites, such as prevascularized subcutaneous device-less sites,[19] or in novel matrices for islet transplantation such as a biofabricated vascularized islet organ.[20] Moreover, the iRFP transgene can be crossed into genetically modified islet donor pig lines to monitor the efficacy of specific modifications in preventing rejection of xeno-islets after transplantation into small and large animal models.

In summary, our data show that pancreatic islets from CAG-iRFP transgenic pigs are fully functional and accessible to long-term monitoring by state-of-the-art imaging modalities. The novel reporter pigs will support the development and preclinical testing of novel matrices and engraftment strategies for porcine xeno-islets.

ACKNOWLEDGMENTS

The authors thank C. Blechinger, T. Schröter (Chair for Molecular Animal Breeding and Biotechnology), and Cheryl Gray (Department of Radiology) for excellent technical support and Heidrun Hirner-Eppeneder (Department of Radiology) for her help performing the MSOT imaging. Some of the data were presented as an abstract at the IXA2019 Congress in Munich, Germany.

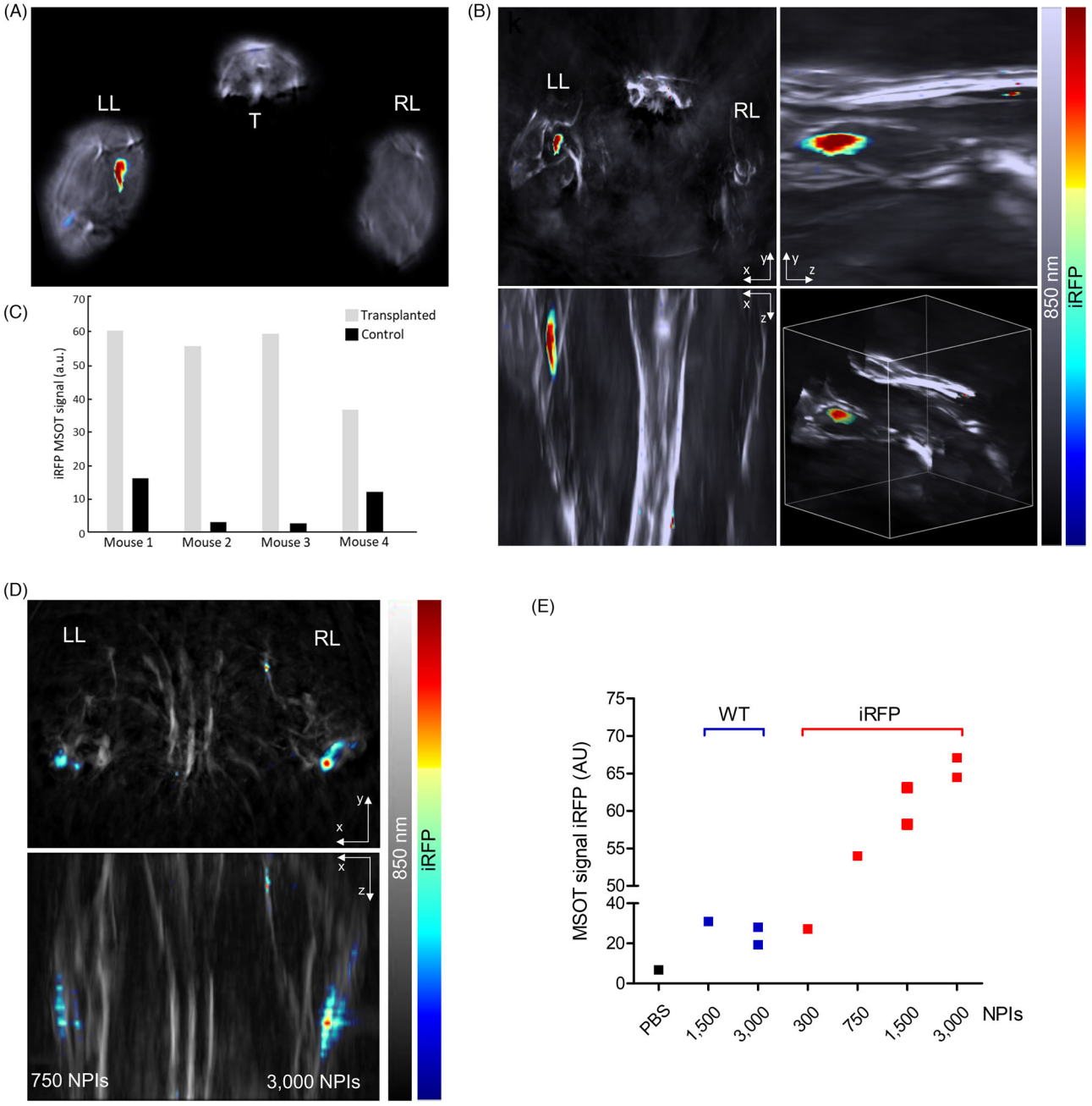

FIGURE 3 Multispectral optoacoustic tomography (MSOT) imaging of iRFP expressing cells in a small recipient model. (A-C) MSOT imaging of CAG-iRFP transgenic NPIs after intramuscular transplantation into the lower hind limbs in STZ-induced diabetic mice after getting normoglycemic. Representative 2D cross-sectional image (A) and 3D images (B). Quantification of the iRFP signal in the left leg (LL) with and the right leg (RL) without islet xenotransplant (C). T = tail. (D,E) MSOT imaging of CAG-iRFP transgenic and WT NPIs 2 days after intramuscular transplantation into the lower hind limbs in STZ-induced diabetic mice. Amount of transplanted NPIs are indicated. (D) Representative 3D images. (E) Quantification of the MSOT signal in the region of interest (ROI).

FUNDING

This project has received funding from the European Union's Horizon 2020 research and innovation programme under grant agreement No. 760986; from the European Union's Horizon2020 research and innovation programme under the Marie Skłodowska Curie grant agreement No. 812660; from the Deutsche Forschungsgemeinschaft (TRR127); from the Bayerische Forschungsstiftung (VasOP; Az. 1247-16), and from the German Federal Ministry of Education and Research (BMBF) to the German Centre for Diabetes Research (DZD e.V.) (grant No. 82DZD00802). The sponsors were not involved in study design and data collection and interpretation.

CONFLICT OF INTEREST

The authors have no conflict of interest to declare.

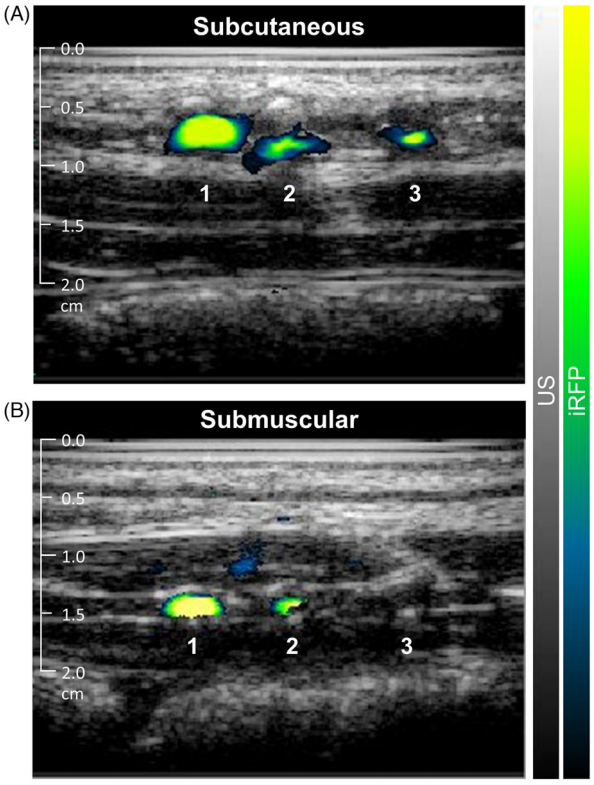

(C)

MSOT signal iRFP (AU)	1	2	3
Subcutaneous	1769	1076	630
Submuscular	731	392	169

FIGURE 4 Multispectral optoacoustic tomography (MSOT) imaging of iRFP expressing cells in a large recipient model. (A-C) MSOT imaging of CAG-iRFP #10105 transgenic NPIs in the subcutaneous (A) and the submuscular (B) layer of the belly of a 14-wk-old pig. NPI density in straws were 1: 66,800 NPI/mL, 2: 17,580 NPIs/mL, and 8,350 NPIs/mL, respectively. (C) MSOT signal iRFP intensity was as indicated. Of note, NPIs sediment quite fast in aqueous suspension as also observed in these straws, influencing and reflected by MSOT imaging dataset.

AUTHOR CONTRIBUTIONS

All authors made substantial contributions to conception and design, acquisition of data, or analysis and interpretation of data. All authors contributed to drafting the article or revising it critically for important intellectual content and provided final approval of the version to be published. EK and EW are the guarantors of this work.

REFERENCES

1. Kemter E, Wolf E. Recent progress in porcine islet isolation, culture and engraftment strategies for xenotransplantation. *Curr Opin Organ Transplant*. 2018;23(6):633-641.
2. Richards TM, Sun A, Hayat H, et al. Current progress and perspective: clinical imaging of islet transplantation. *Life (Basel)*. 2020;10(9):213.
3. Kemter E, Cohrs CM, Schäfer M, Schuster M, Steinmeyer K, Wolf-van Buerck L, Wolf A, Wuensch A, Kurome M, Kessler B, Zakhartchenko V, Loehn M, Ivashchenko Y, Seissler J, Schulte AM, Speier S, Wolf E. INS-eGFP transgenic pigs: a novel reporter system for studying maturation, growth and vascularisation of neonatal islet-like cell clusters. *Diabetologia*. 2017;60:(6):1152–1156. http://doi.org/10.1007/s00125-017-4250-2
4. Cohrs CM, Chen C, Jahn SR, et al. Vessel network architecture of adult human islets promotes distinct cell-cell interactions in situ and is altered after transplantation. *Endocrinology*. 2017;158(5):1373-1385.
5. Karasev MM, Stepanenko OV, Rumyantsev KA, Turoverov KK, Verkhusha VV. Near-infrared fluorescent proteins and their applications. *Biochemistry (Mosc)*. 2019;84(Suppl 1):S32-S50.
6. Chinnathambi S, Shirahata N. Recent advances on fluorescent biomarkers of near-infrared quantum dots for in vitro and in vivo imaging. *Sci Technol Adv Mater*. 2019;20(1):337-355.
7. Wang LV, Hu S. Photoacoustic tomography: in vivo imaging from organelles to organs. *Science*. 2012;335(6075):1458-1462.
8. Regensburger AP, Fonteyne LM, Jungert J, et al. Detection of collagens by multispectral optoacoustic tomography as an imaging biomarker for Duchenne muscular dystrophy. *Nat Med*. 2019;25(12):1905-1915.
9. Schellenberg MW, Hunt HK. Hand-held optoacoustic imaging: a review. *Photoacoustics*. 2018;11:14-27.
10. Shcherbakova DM, Verkhusha VV. Near-infrared fluorescent proteins for multicolor in vivo imaging. *Nat Methods*. 2013;10(8):751-754.
11. Weinberg BH, Pham NTH, Caraballo LD, et al. Large-scale design of robust genetic circuits with multiple inputs and outputs for mammalian cells. *Nat Biotechnol*. 2017;35(5):453-462.
12. Richter A, Kurome M, Kessler B, et al. Potential of primary kidney cells for somatic cell nuclear transfer mediated transgenesis in pig. *BMC Biotechnol*. 2012;12:84.
13. Kurome M, Kessler B, Wuensch A, Nagashima H, Wolf E. Nuclear transfer and transgenesis in the pig. *Methods Mol Biol*. 2015;1222:37-59.
14. Klymiuk N., van Buerck L., Bahr A., Offers M., Kessler B., Wuensch A., Kurome M., Thormann M., Lochner K., Nagashima H., Herbach N., Wanke R., Seissler J., Wolf E.. Xenografted Islet Cell Clusters From INSLEA29Y Transgenic Pigs Rescue Diabetes and Prevent Immune Rejection in Humanized Mice. *Diabetes*. 2012;61:(6):1527–1532. http://doi.org/10.2337/db11-1325
15. Wolf-van Buerck L, Schuster M, Baehr A, et al. Engraftment and reversal of diabetes after intramuscular transplantation of neonatal porcine islet-like clusters. *Xenotransplantation*. 2015;22(6):443-450.
16. Dinnyes A, Schnur A, Muenthaisong S, et al. Integration of nano- and biotechnology for beta-cell and islet transplantation in type-1 diabetes treatment. *Cell Prolif*. 2020;53(5):e12785.
17. Arifin DR, Bulte JWM. In vivo imaging of pancreatic islet grafts in diabetes treatment. *Front Endocrinol (Lausanne)*. 2021;12:640117.
18. Hornblad A, Ahlgren U. Optical imaging of islets: new possibilities by the development of infrared fluorescent proteins. *Islets*. 2009;1(2):163-164.
19. Pepper AR, Gala-Lopez B, Pawlick R, Merani S, Kin T, Shapiro AM. A prevascularized subcutaneous device-less site for islet and cellular transplantation. *Nature Biotechnol*. 2015;33(5):518-523.
20. Citro A, Moser PT, Dugnani E, et al. Biofabrication of a vascularized islet organ for type 1 diabetes. *Biomaterials* 2019;199:40-51.

SUPPORTING INFORMATION

Additional supporting information may be found in the online version of the article at the publisher's website.

How to cite this article: Kemter E, Citro A, Wolf-van Buerck L, et al. Transgenic pigs expressing near infrared fluorescent protein—A novel tool for non-invasive imaging of islet xenotransplants. *Xenotransplantation*. 2021; e12719. https://doi.org/10.1111/xen.12719